

Supplemental Table S1. Antibodies used.

	Vendor	Catalog number	Dilution
Western Blot Antibodies			
Snip3	Cell Signaling	3769	1:1000
GAPDH	Cell Signaling	5174	1:1000
LC3A/B	Cell Signaling	12741	1:1000
NDUSF1	Abcam	102552	1:1000
OXPHOS	Abcam	110413	1:1000
p-4ebp1 (Thr37/46)	Cell Signaling	2855	1:1000
p-S6 (Ser235/236)	Cell Signaling	2211	1:1000
S6	Cell Signaling	2317	1:1000
UbiquitinK48	Abcam	190061	1:1000
p-ULK⁵⁵⁵	Cell Signaling	5869	1:1000
Anti-Puromycin Sera (non-concentrated)	DSHB University of Iowa	PMY-2A4-S	1:20
ULK1	Cell Signaling	8054	1:500
VDAC	Cell Signaling	4866	1:1000
Peroxidase Anti-Mouse IgG (secondary Ab)	Jackson ImmunoResearch	115-035-208	1:10,000
Rabbit secondary antibody	Thermo Fisher	SA5-35571	1:10,000
Mouse secondary antibody	Thermo Fisher	SA5-35521	1:10,000
Immunofluorescence Antibodies			
Laminin	Sigma	L9393	1:100
LC3A	Cell Signaling	4599	1:200
Myosin IIa	DSHB University of Iowa	SC-71	1:250
Myosin heavy chain, slow (Type I and IIa)	DSHB University of Iowa	BA-F8	1:250
Alexa-Fluor-555 Goat anti mouse	Thermo Fisher	A-21147	1:500
Alexa-Fluor-647 Goat anti mouse	Thermo Fisher	A-32728	1:200
Alexa-Fluor-488 Goat anti Rabbit	Thermo Fisher	A-11008	1:500

Supplemental Table S2. Primers for quantitative RT-PCR of mouse genes.

Common name	Gene name	5' primer	3' primer
4E-Bp	<i>Eif4ebp1</i>	CCTCCTTGTGCCTGTGTCTA	GCCTAAGGAAAGATGGGTGT
Atp5c1	<i>Atp5c1</i>	CCAGGAGACTGAAGTCCATCA	AGAACCTGTCCCATACTCG
Atrogin-1	<i>Fbxo32</i>	CTGTGCTGGTGGGCAACATTAACA	CGTCACTCAGCCTCTGCATGAT
Bnip3	<i>Bnip3</i>	CCCAGACACCACAAGATACCAACA	GGTCGACTTGACCAATCCCATATCCA
Bnip3L	<i>Bnip3l</i>	CACCACAAGAAGATGGGCAGATCA	TGGACCAGTCTGATACCCAGT
Cathepsin L	<i>Ctsl</i>	TATCCCTCAGCAAGAGAAAGCCCT	TCCTTCATAGCCATAGCCCACCAA
Cox5b	<i>Cox5b</i>	GGAAGACCCTAATCTAGTCCCG	GTTGGGGCATCGCTGACTC
FoxO1	<i>Foxo1</i>	TGCTGTGAAGGGACAGATTG	GAGTGGATGGTGAAGAGCGT
FoxO3	<i>Foxo3</i>	ACAAACGGCTCACTTTGTCCAGA	TCTTGCCCGTGCCTTCATTCT
FoxO4	<i>Foxo4</i>	GGTGCCCTACTTCAAGGACA	AGCTTGCTGCTGCTATCCAT
Gabarapl	<i>Gabarapl1</i>	GTCATCGTGGAGAAGGCTCCTAAA	GGAGGGATGGTGTGTTGACAAAAG
Gadd45a	<i>Gadd45a</i>	GGATCCTTCCATTGTGATGAA	TGCTACTGGAGAACGACGC
Itch	<i>Itch</i>	CCACCCACCCACGAAGACC	CTAGGGCCCGAGCCTCCAGA
Lamp2a	<i>Lamp2</i>	ACAACCTGACTCCTGTCTGTTGAGA	AGTTGGAGTTGGAGTGGGTGTTGA
LC3A	<i>Map1lc3a</i>	TCTGGTCCCAGACCATGTTA	GGTTGACCAGCAGGAAGAAG
LC3B	<i>Map1lc3b</i>	CACTGCTCTGTCTTGTGTAGTTG	TCGTTGTGCCTTTATTAGTGCATC
MuRF-1	<i>Trim63</i>	ATGAAGTGATCATGGACCGCA	TTGCACAAGGAGCAAGTAGGCA
MUSA1	<i>Fbxo30</i>	TCGTGGAATGGTAATCTTGC	CCTCCCGTTTCTCTATCACG
Ndufs1	<i>Ndusf1</i>	TGCAAATCCCTCGATTCTGTTAC	GCTTTCTCAATCTCTACCAGGC
Ndusf2	<i>Ndusf2</i>	TCGTGCTGGAAGTGAAGTGA	GGCCTGTTTATTACACATCATGG
Ndufb8	<i>Ndufb8</i>	CCCGCTCCAGGTACAGATTA	GCTTTGTGGCTTTTATGTTT
Ndufv1	<i>Ndufv1</i>	GTGCGGGTATCTGTGCGTT	GGTTGGTAAAGATCCGGTCTTC
p27 Kip1	<i>Cdkn1b</i>	GGGGAACCGTCTGAAACATT	AGTGTCCAGGGATGAGGAAG
Psme4	<i>Psme4</i>	AATTTTCTCCATAAAGTCGGA	CAGATCAAGAGCAACCTGGG
Sdha	<i>Sdha</i>	GCTTGCGAGCTGCATTTGG	TGTGATCGGGTAGGAAAGAGC
Sdhb	<i>Sdhb</i>	TCTGGGTCCCATCGGTAAAT	GCCGTTCTCGGCAGAGTC
SMART	<i>Fbxo21</i>	TCAATAACCTCAAGGCGTTC	GTTTTGCACACAAGCTCCA
TBP	<i>Tbp</i>	ACCCTTACCAATGACTCCTATG	TGACTGCAGCAAATCGCTTGG
Ube4a	<i>Ube4a</i>	GTTTGCAGCAATCCAGAAAGAG	CAGGCTCTGACACACTATTATC
Ulk1	<i>Ulk1</i>	TGCAAATGGTACAATCAGCTGCC	AGCAGGGCTTTGTGATATCTCGGT
Uqcrc2	<i>Uqcrc2</i>	GATAACCCGTGGGATTGAAGC	TCTACAGTGTACGCCATGTTTTC

Supplemental Table S3. CalR statistics for indirect calorimetry. GLM model was used.

	<i>Mass</i> Pr(> t)	<i>Group TKO</i> Pr(> t)	<i>Mass:Group TKO</i> Pr(> t)
Oxygen Consumption (ml/hr)	0.1342	0.5968	0.5212
Carbon Dioxide Production (ml/hr)	0.2501	0.4853	0.4251
Energy Expenditure (kcal/hr)	0.1527	0.5644	0.4922
Total Energy Expenditure (kcal)	0.1227	0.6194	0.5213
Respiratory Exchange Ratio	-	0.1069	-
Food Consumed (kcal/hr)	0.9554	0.6529	0.6198
Total Food Consumed (kcal)	0.9553	0.7624	0.7411
Water Consumed (ml/hr)	0.8491	0.7296	0.6580
Total Water Consumed (ml)	0.7772	0.6600	0.5997
Locomotor Activity (beam breaks/hr)	-	0.4804	-
Pedestrian Locomotion (m)	-	0.0571	-
Total Distance in Cage (m)	-	0.0265*	-
Total Body Mass (g)	0.099	0.1558	0.1427

Supplemental Figure S1. Muscle-specific FoxO deletion increases lean percent and liver weight with aging but does not change survival. Quantitative RT-PCR of FoxO1, FoxO3, and FoxO4 in quadriceps muscle (a) (n= 9-13 per group). Percent body fat and percent lean from NMR in Figure 1, panel A (b) (n=10-14 per group). Liver (c) heart (d), iWAT, pg-WAT, and BAT (e) weights of young (4.5 months), and aged (24 months) male TKO and littermate control mice (n=10-14 per group). Kaplan Meier survival curve (f) of aged groups from start to end of study (n=15-19 control vs. TKO). *= $p < 0.05$, **= $p < 0.01$ as indicated by 2-way ANOVA. (iWAT- inguinal white adipose tissue, pg-WAT- perigonadal white adipose tissue, BAT- brown adipose tissue).

Supplemental Figure S2. FoxO deletion in muscle mildly increases fiber size and markedly increases fibers with central nuclei in plantaris, but does not cause myofiber necrosis. Laminin stain of plantaris muscle cross section (scale bar 250 μ m) (a). Distribution of cross-sectional area of plantaris fibers from Laminin staining in panel a (b). Quantification of central nuclei (c) and total number of nuclei in plantaris from panel a (d). (n=5-6 per group). Representative H&E stain (e) of TA and soleus muscle from each group (scale bar 200 μ m). Representative IgM and IgG stain (scale bar 200 μ m) (f) of TA and soleus muscle from each group (n=8-13 per group with no positive internal staining). HPF= High power field. *= $p < 0.05$ as indicated. ^ = $p < 0.05$ genotype main effect. # = $p < 0.05$ age main effect by 2-way ANOVA.

Supplemental Figure S3. FoxO deletion decreases autophagy-lysosome genes and ULK1 levels and phosphorylation in Young and Aged TKO muscle. Quantitative RT-PCR of autophagy lysosomal genes (a) from young Ctrl, Young TKO, Aged Ctrl, and Aged TKO quadriceps muscle. (n=9-13 per group). TBP was used as a housekeeping normalizer. Autophagy proteins measured

by western blot in quad muscle (b). Densitometry of indicated proteins from panel b (c, d). (n=6 per group). *= $p < 0.05$, **= $p < 0.01$ as indicated, ^= $p < 0.05$ genotype main effect by 2-way ANOVA.

Supplemental Figure S4. Protein synthesis and Autophagy flux are unchanged in Young TKO after post-prandial 6-hour fast. Protein synthesis measured by SUNsET method of puromycin incorporation in quad, TA, and soleus muscle from Young Ctrl saline, Young Ctrl colchicine, Young TKO saline, and Young TKO colchicine mice. Anti-Puromycin western blot (a-c) and densitometry (d-f) in quad, TA and soleus (n= 4-6 per group). Autophagy flux was measured by western blot of LC3 and Bnip3 in quad, TA, and soleus muscle. Western blot and Densitometry (g-i) of Bnip3 and LC3 from Young Ctrl saline, Young Ctrl colchicine, Young TKO saline, and Young TKO colchicine (n=4-6 per group). *= $p < 0.05$, **= $p < 0.01$ as indicated, \$= $p < 0.05$ treatment main effect, \$\$= $p < 0.01$ treatment main effect by 2-way ANOVA.

Supplemental Figure S5. Whole-body metabolism is minimally changed in aged FoxO-TKO mice relative to aged controls. Energy expenditure over time and averaged for dark and light cycles during indirect calorimetry experiments (a). Respiratory quotient, and respiratory quotient per mouse for dark and light cycles (b). Total distance in cage (c), and average food intake (d), . (n= 6 control, and 8 TKO mice per group). Data collected in Aged Ctrl and Aged TKO mice by indirect calorimetry over 48 h ad libitum feeding (40-hour acclimation period was done before displayed measurements). $p < 0.05$ aged control vs. aged TKO by Cal-R analysis (see Supplemental Table 3 for statistics.)

Supplemental Figure S6. Respiration and ATP production in isolated muscle mitochondria decreases with age. Basal, submaximal (5 and 10 μM ADP) and maximal (1000 μM ADP) respiration in isolated mitochondria from mixed quad/gastrocnemius using Glutamate/Malate (Glu/M) substrates (a). ATP production of isolated mitochondria using Glu/M substrates a various ADP concentration (b) (n = 4-13 per group). * = $p < 0.05$ young vs. aged in the same group, # = $p < 0.05$ age main effect by 2-way ANOVA.

Supplemental Figure S7. Fiber type and mitochondrial cristae are not affected by aging or FoxO deletions in plantaris. Quantification of percent of muscle fibers from succinate dehydrogenase (SDH) stained plantaris muscle (a) (n=5-6 per group). Transmission Electron Microscopy images (b) and quantification (c) of mitochondria cristae graded using cristae score based on reference #36 (Eisner V. PNAS 2017) (scale bar = 400 nm). See Methods for details. Images of myosin-stained fibers in plantaris muscle (d) (scale bar 500 μM). Quantification of percent (e) of myosin fibers in plantaris muscle (n=5-6 per group). $\wedge = p < 0.05$ genotype main effect and #= $p < 0.05$ age main effect by 2-way ANOVA.

Supplemental Figure S8. Changes in myosin fiber types with ageing and FoxO deletion in TA and Soleus muscle. Images of myosin-stained fibers in TA (a), and soleus (c) muscle (scale bar = 500 μm). Quantification of percent of myosin-stained fibers in TA (b) and soleus (d) muscle. Average CSA of type I (e), and type IIa (f) in soleus muscle. (n=10-11 per group). *= $p < 0.05$, **= $p < 0.01$ as indicated, \wedge genotype main effect, # = $p < 0.05$ age main effect by 2-way ANOVA.

Supplemental Figure S9. Mitochondrial protein levels in young and aged TKO mice. NDUFS1 and VDAC measured by western blot in quad muscle tissue lysates (a). Densitometry of NDUFS1 (b), and densitometry of VDAC (c) (n=9-13 per group). OXPHOS subunits measured by western blot in TA muscle (d). Densitometry of indicated subunit from complexes I, III, IV and V (e) shown in panel d (n=5-6 per group). *= $p < 0.05$, **= $p < 0.01$ as indicated; #= $p < 0.05$ age main effect by 2-way ANOVA.

Supplemental Methods

Grip strength test. Forelimb grip strength was determined using a grip strength meter equipped with a triangular pull bar (Columbus Instruments). Each mouse was subjected to 2 rounds of 3 consecutive tests to obtain the peak value over a period of 2 days.

Exercise tolerance test (ETT). ETT were performed as previously described [1]. After acclimation, ETT was performed by placing the treadmills at a 10° angle and the starting speed at 4m/min then increasing the treadmill speed by 2m/min every 10 minutes for 70 minutes. After 70 minutes speed was increased by 4m/min every 10 minutes until exhaustion, determined by the mice being unable to leave the treadmill shock grids for 10 consecutive seconds. Shock grids were set to irritate but not harm the mice.

In vivo muscle contractile function. TA muscle function was assessed by stimulating the common fibular nerve to induce tetanic and maximal isometric contractions of ankle dorsiflexors as previously described [2]. Mice were maintained under isoflurane anesthesia on a warming platform kept at 35°C. The knee of the mouse was secured between pivots, and the foot was placed in and secured to the foot plate attached to a force transducer. A total of 2 needle electrodes (monopolar polytetrafluoroethylene-coated stainless steel) (Chalgren Enterprises, Gilroy, CA, USA) were used for percutaneous stimulation of the common fibular nerve. Tetanic isometric contractions at optimal length were elicited by stimulations of 150Hz for 300ms using the 1300A 3-in-1 Whole Animal System (1300A; Aurora Scientific, Aurora, ON, Canada). Data were collected and analyzed to determine muscle torque using the Dynamic Muscle Analysis software (ASI 611A v.5.321; Aurora Scientific).

IgG and IgM Immunofluorescence: IgG and IgM staining was performed as previously described [3]. Briefly frozen muscle sections of quad, TA, and soleus muscle were preincubated for 30 minutes with 5% BSA in PBS, followed by a 1-hour incubation with goat anti mouse IgM, or IgG antibodies. Sections were then washed in PBS with 0.1% tween, and mounted with ProLong Gold antifade mounting media.

Proteasome Activity Assays: Proteasome activity was determined in 20 µg of quadriceps muscle homogenates. using substrates for peptidyl-glutamyl-like and trypsin-like activity of the 26S proteasome as previously described [4, 5], with the following modifications: Z-Leu-Leu-Glu-7-amido-4-methylcoumarin (LLE) (C0483; Sigma-Aldrich) and Boc-Leu-Ser-Thr-Arg-7-amido-4-methylcoumarin (LSTR) (B4636; Sigma) were both used at 300 µmol/L final concentrations in separate assays. Enzyme activity (V_{max}) was determined as the change in fluorescence during the linear phase of the reaction without MG132 minus the activity with 200 µmol/L MG132, each converted to nanomoles per minute per milligram using a standard curve of 7-amido-4-methylcoumarin (A9891; Sigma-Aldrich).

Protein Synthesis Assay: Muscle protein synthesis was measured using the SUnSET (surface sensing of translation) method as previously described [6]. Briefly, mice were fasted for 6 hours then 0.04 µmol/g puromycin dissolved in PBS was intraperitoneally administered. 30 minutes after the puromycin injections, muscles were extracted and snap frozen. Western blotting was done in tissue homogenate using anti-puromycin antibody. Peroxidase anti-mouse IgG secondary antibody was used, and chemiluminescent ECL western blotting substrate (Thermo Scientific) was used to develop these blots.

Autophagy flux Analysis: To measure autophagy flux an autophagy inhibitor Colchicine (0.4 mg/kg/d; Sigma Aldrich) or saline was intraperitoneally administered in mice for 3 days as previously described [6]. After the third day of colchicine treatment muscle were harvested, and western blotting was performed for selected autophagy markers.

Indirect calorimetry. Aged mice were individually housed in Promethion metabolic cages (Sable Systems) for 5 days with ad libitum access to food and water. During the first 40 h of acclimation, data were recorded, but excluded from the analysis. Indirect calorimetry data was analyzed using CalR: A Web-based Analysis Tool for Indirect Calorimetry Experiments (<https://calrapp.org/>) [7] and presented in Supplemental table S3.

Mitochondrial Function Assays. Briefly, plantaris muscles were dissected and immediately placed into ice cold Buffer X containing 7.23 mM K₂EGTA, 2.77 mM CaK₂EGTA, 20 mM Imidazole, 0.5 mM DTT, 20 mM Taurine, 5.7 mM ATP, 14.3 mM creatine monophosphate, 6.56 mM MgCl₂-6H₂O, 50 mM MES (2-(N-morpholino) ethanesulfonic acid), pH to 7.1. Fibers were manually dissociated and separated into bundles using blunted needles under a dissecting microscope, then permeabilized in Buffer X containing 50 µg/ml saponin for 40 minutes. Fiber bundles were placed in Buffer Z containing 105 mM K-MES, 30 mM KCl, 10 mM KH₂PO₄, 5 mM MgCl₂-6H₂O, 2.5 mg/ml BSA, 1mM EGTA, 20 µM Blebbistatin, 20 mM Creatine monohydrate, pH 7.4 on ice until use. For respiration measurements, fibers (~2-4 mg) were placed in 2.5 mL of Buffer Z at 30°C, and respiration was determined in an Oroboros oxygraph with the following substrates (as indicated in figures) and concentrations: 2 mM Malate, 5 mM Pyruvate, 20 µM Palmitoyl-carnitine, 5 mM Glutamate, ADP concentration indicated in figures, 5 mM Succinate,

10 μ M Rotenone, 10 μ g/mL Oligomycin, 10 μ M FCCP. ATP production was measured in Buffer Z containing 0.5 mg/ml BSA instead of 2.5 mg/ml. To monitor ATP production, ATP was converted to NADPH by addition of 4 mM glucose, 200 μ M NADP⁺ (Sigma N0505), 50 μ M P¹, P⁵-Di(adenosine-5') pentaphosphate pentasodium salt (Sigma D4022), and 10 μ L/mL of a Hexokinase/Glucose-6-Phosphate Dehydrogenase mixture (Sigma 10127825001) to Buffer Z and monitored in a Horiba fluorometer Ex/Em (345nm/460nm). Respiration of isolated mitochondria in the first aged cohort was performed using 75 μ g/mL of mitochondrial protein in "Respiration Buffer" containing 120 mM KCl, 5 mM KH₂PO₄, 2 mM MgCl₂, 1 mM EGTA, 3 mM HEPES, 0.3% BSA fatty acid free, pH 7.2, as described previously [8]. Please note that the respiration of isolated mitochondria of the first aged cohort was performed in Buffer Z containing BSA 2.5 mg/ml. These samples were not included in the final analysis, however the data from these samples showed a similar trend as the data shown, but excluded due to being placed in a different buffer.

Citrate synthase, Complex I and Complex II Enzymatic assays. Briefly, citrate synthase (CS) was measured using 5 μ g of Tibialis anterior (TA) protein in a final solution of 200 μ l containing 200 mM Tris with a pH of 8.0, 0.2% vol/vol Triton X-100, 100 mM of 5, 5-Dithiobis (2-nitrobenzoic acid) (DTNB), 10 mM Acetyl-CoA, and 0.5 mM oxaloacetic acid which started the reaction. The reaction was monitored for an increase in absorbance at 412 nm for 3 min. Complex I was measured using 40 μ g of TA protein in a final solution of 200 μ l containing 0.5 M potassium phosphate with a pH of 7.5, 50 mg ml⁻¹ of fatty acid free BSA, 10 mM KCN, with or without 10 mM rotenone to check for specificity, and 10 mM of ubiquinone₁ which started the reaction. The reaction was monitored for a decrease in absorbance at 340 nm for 8 minutes. Complex II

was measured using 10 ug of TA protein in a final solution of 200 ul containing 0.5M potassium phosphate with a pH of 7.5, 50 mg ml⁻¹ of fatty acid free BSA, 10 mM KCN, 400 mM Succinate, 0.015% wt/vol of 2,6-dichlorophenolindophenol sodium salt hydrate (DCPIP), with or without 1 M malonate to check for specificity, and 12.5 mM decylubiquinone (DUB) to start the reaction. The reaction was monitored for a decrease in absorbance at 600nm for 5 minutes.

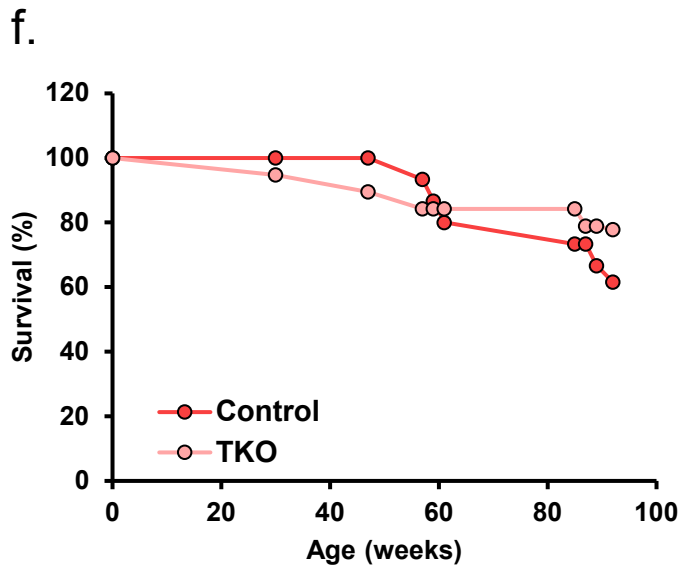
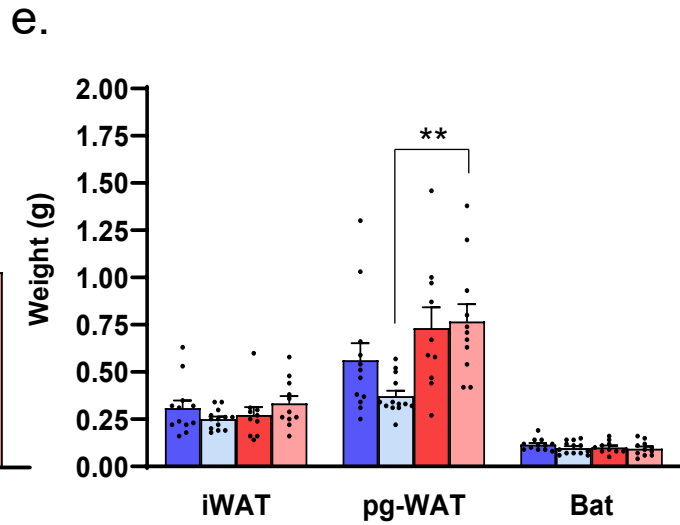
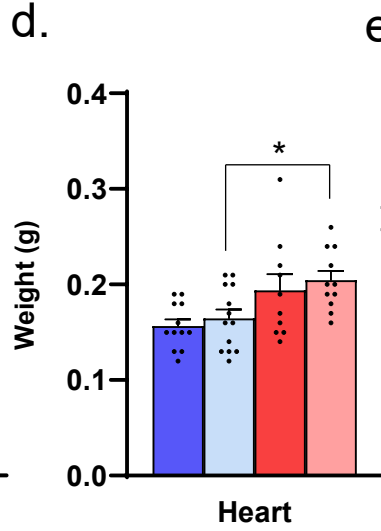
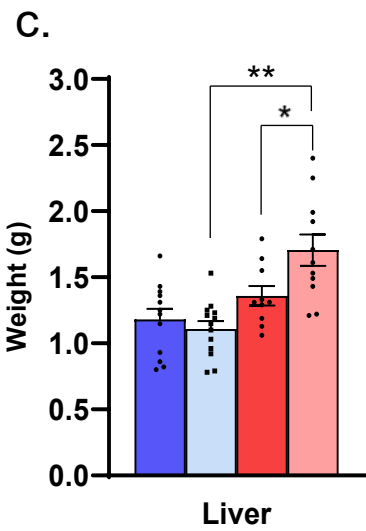
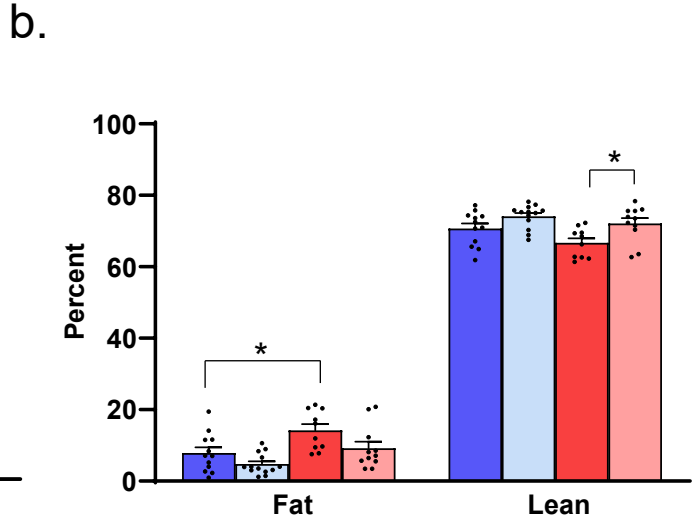
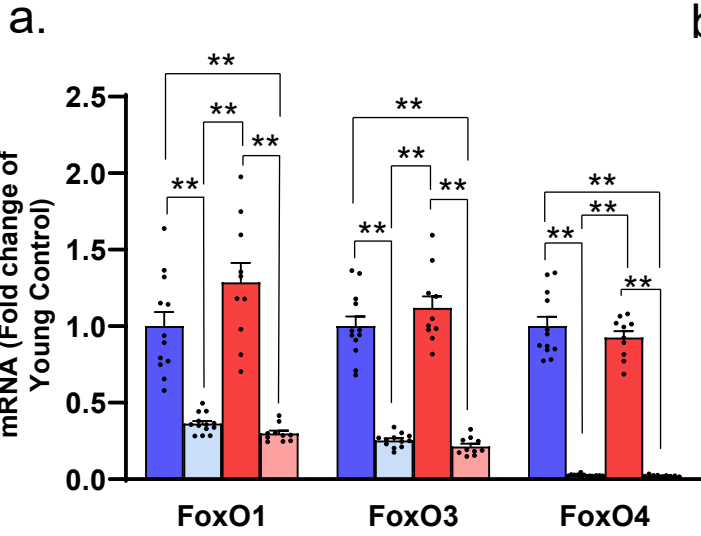
Serum Insulin Quantification. Serum insulin concentrations were measured using Crystal Chem Ultra-Sensitive Mouse Insulin ELISA Kit (Catalog # 90080), according to the manufacturer's protocol.

Supplemental References

1. Sharma, A., et al., *Impaired skeletal muscle mitochondrial pyruvate uptake rewires glucose metabolism to drive whole-body leanness.* Elife, 2019. **8**.
2. Fuqua, J.D., et al., *ULK2 is essential for degradation of ubiquitinated protein aggregates and homeostasis in skeletal muscle.* FASEB J, 2019. **33**(11): p. 11735-11745.
3. Straub, V., et al., *Animal models for muscular dystrophy show different patterns of sarcolemmal disruption.* J Cell Biol, 1997. **139**(2): p. 375-85.
4. O'Neill, B.T., et al., *Insulin and IGF-1 receptors regulate FoxO-mediated signaling in muscle proteostasis.* J Clin Invest, 2016. **126**(9): p. 3433-46.
5. Kisselev, A.F. and A.L. Goldberg, *Monitoring activity and inhibition of 26S proteasomes with fluorogenic peptide substrates.* Methods Enzymol, 2005. **398**: p. 364-78.
6. Bhardwaj, G., et al., *Insulin and IGF-1 receptors regulate complex-I dependent mitochondrial bioenergetics and supercomplexes via FoxOs in muscle.* J Clin Invest, 2021.
7. Mina, A.I., et al., *CalR: A Web-Based Analysis Tool for Indirect Calorimetry Experiments.* Cell Metab, 2018. **28**(4): p. 656-666 e1.
8. Yu, L., et al., *Mitochondrial function in diabetes: novel methodology and new insight.* Diabetes, 2013. **62**(6): p. 1833-42.

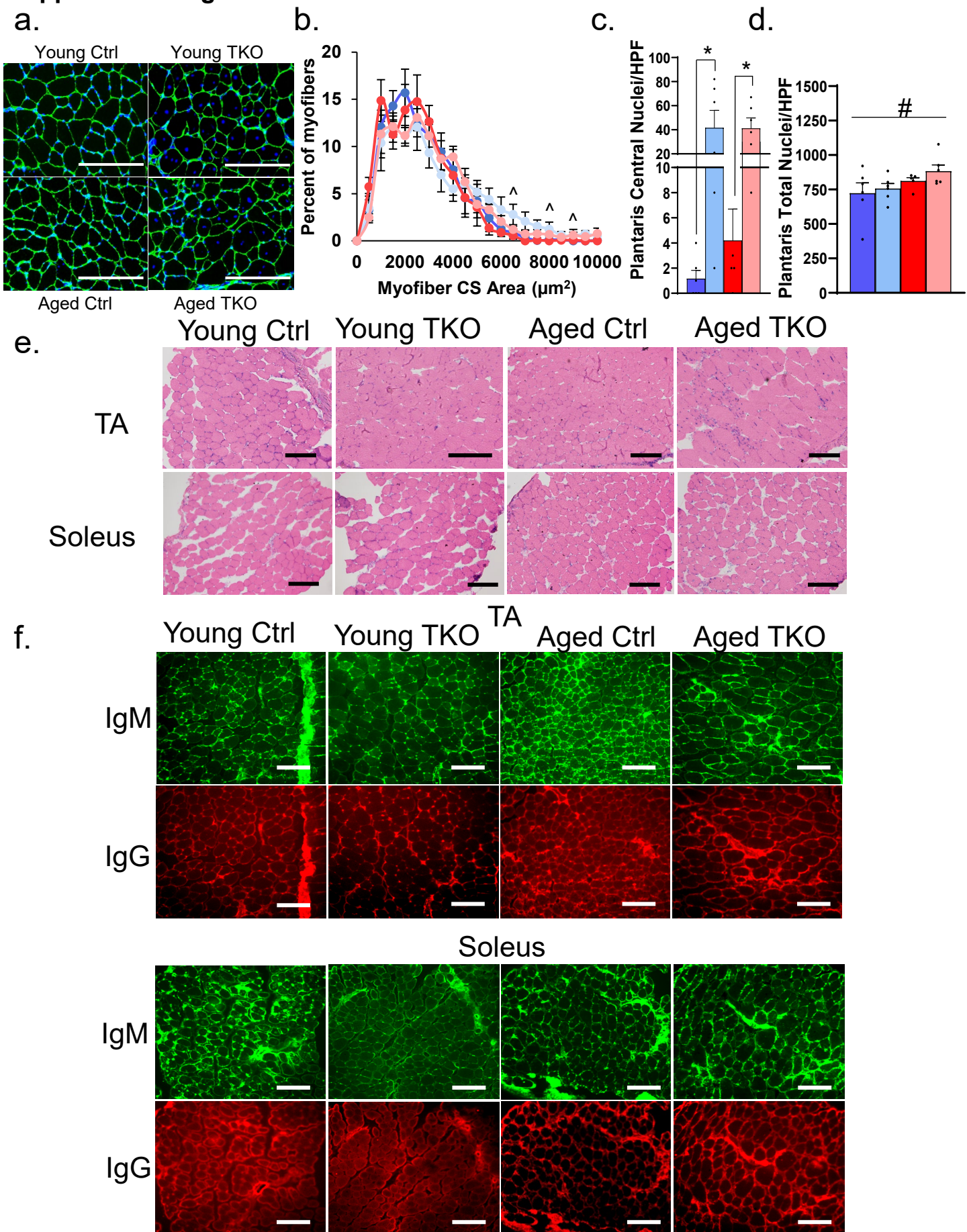
Supplemental Figure S1

■ Young Ctrl
 ■ Young TKO
 ■ Aged Ctrl
 ■ Aged TKO



Supplemental Figure S2

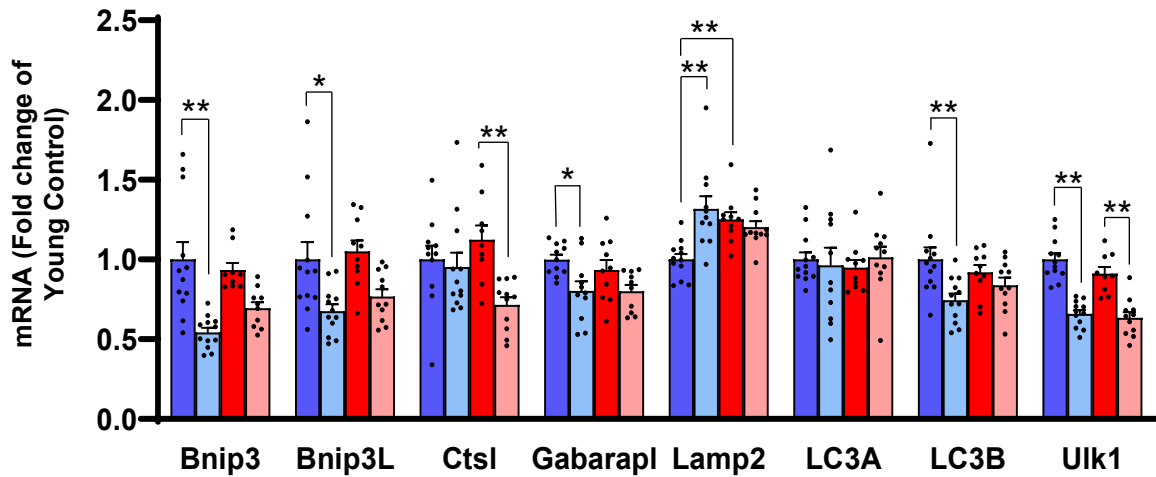
■ Young Ctrl
 ■ Young TKO
 ■ Aged Ctrl
 ■ Aged TKO



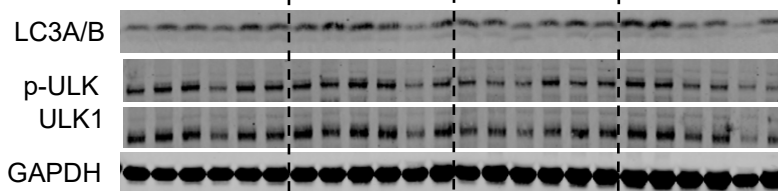
Supplemental Figure S3

■ Young Ctrl ■ Young TKO ■ Aged Ctrl ■ Aged TKO

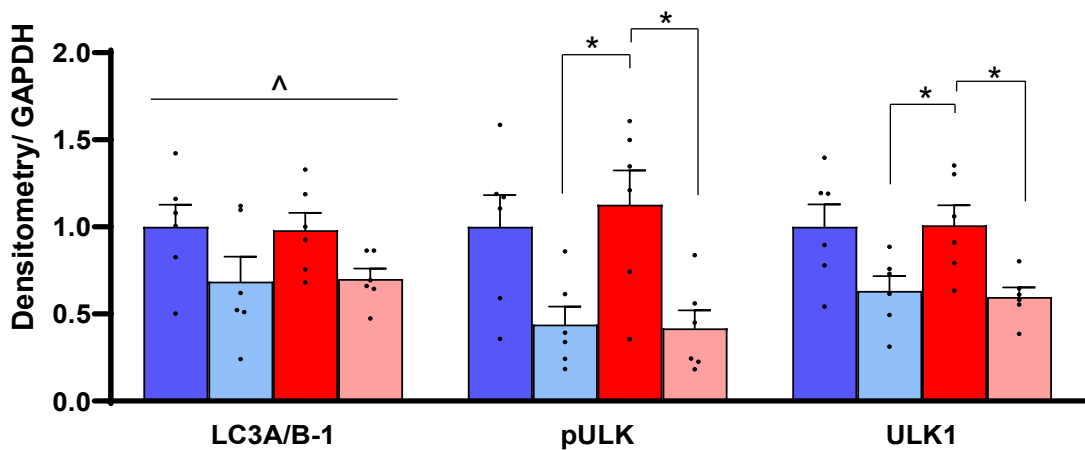
a. Quad Autophagy and Lysosomal Genes



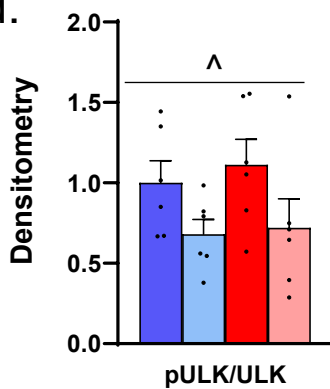
b. Control Aged Young TKO Aged Young



c.

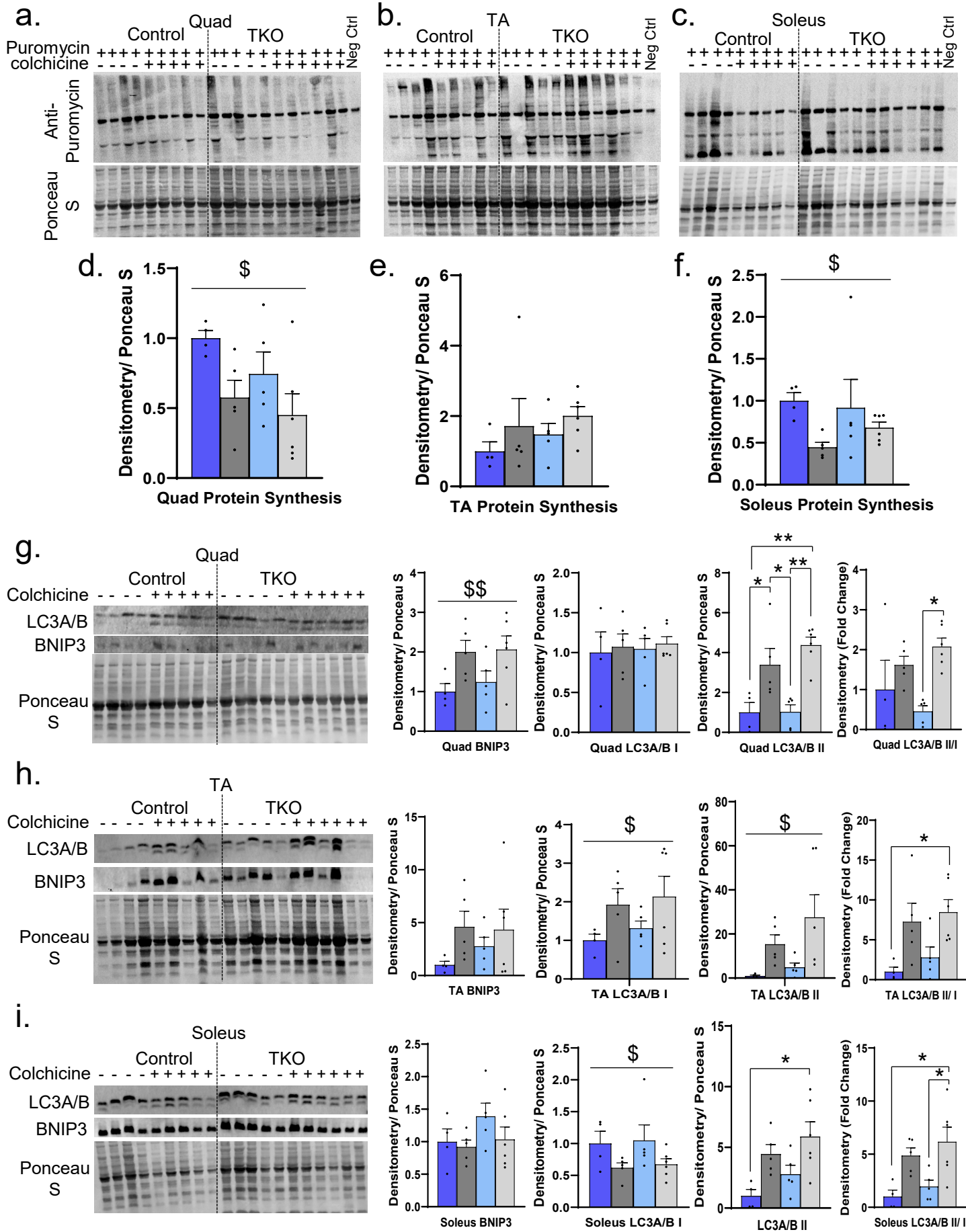


d.



Supplemental Figure S4

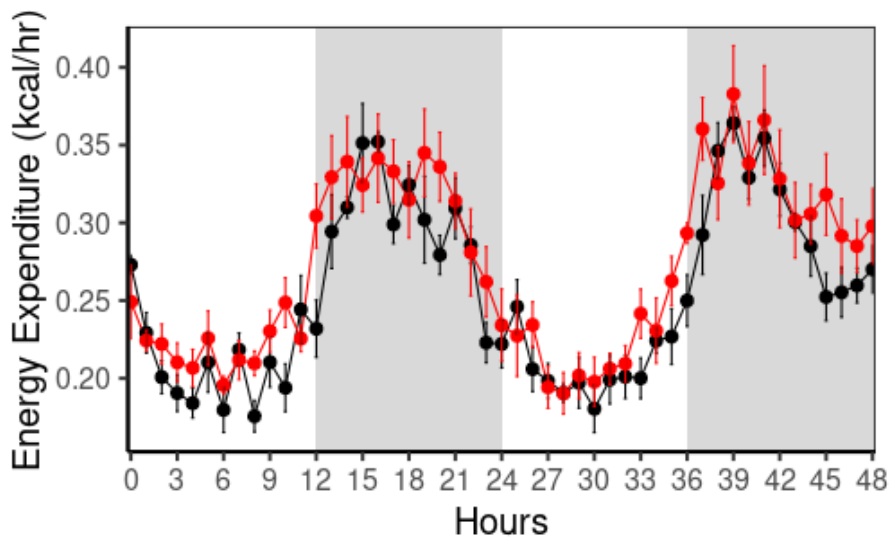
■ Ctrl Saline
 ■ Ctrl Colchicine
 ■ TKO Saline
 ■ TKO Colchicine



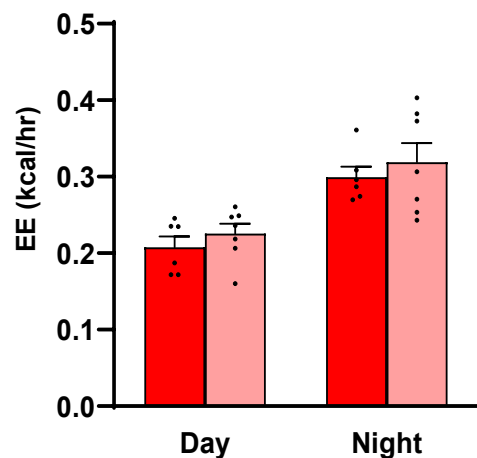
Supplemental Figure S5

● Aged Ctrl ● Aged TKO ■ Aged Ctrl ■ Aged TKO

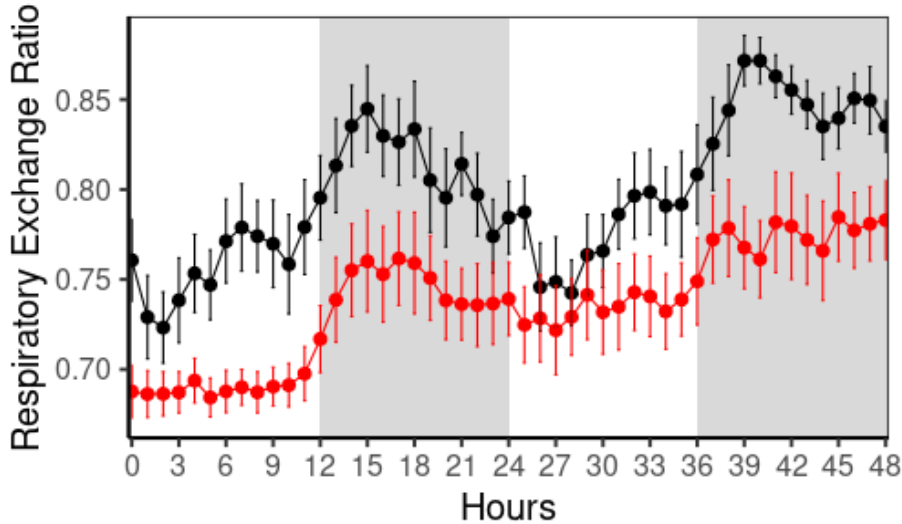
a.



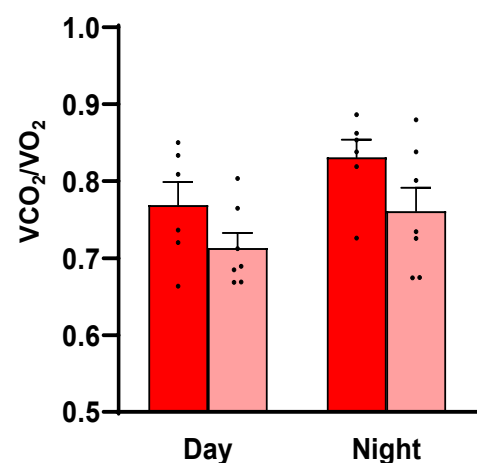
Energy Expenditure



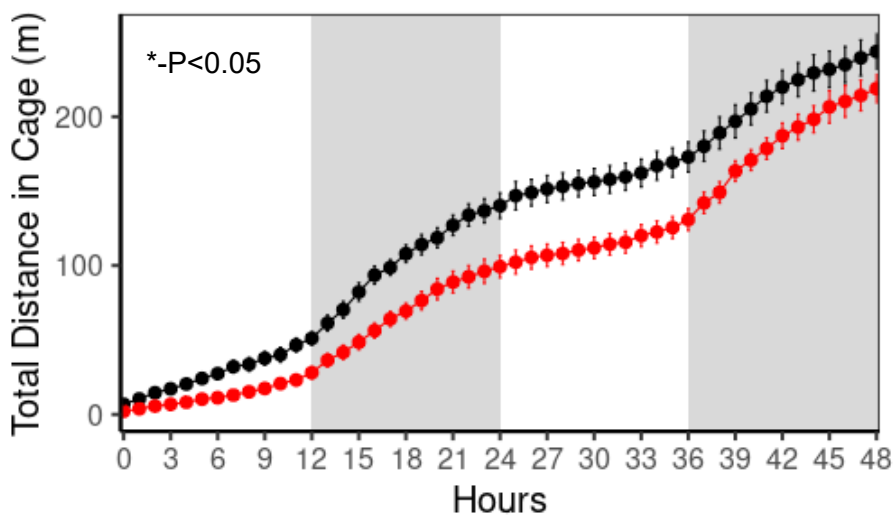
b.



Respiratory Exchange Ratio

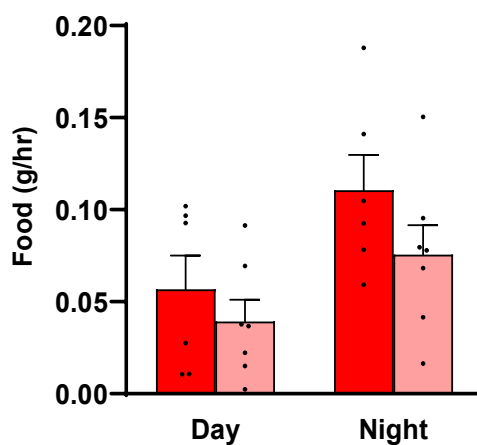


c.

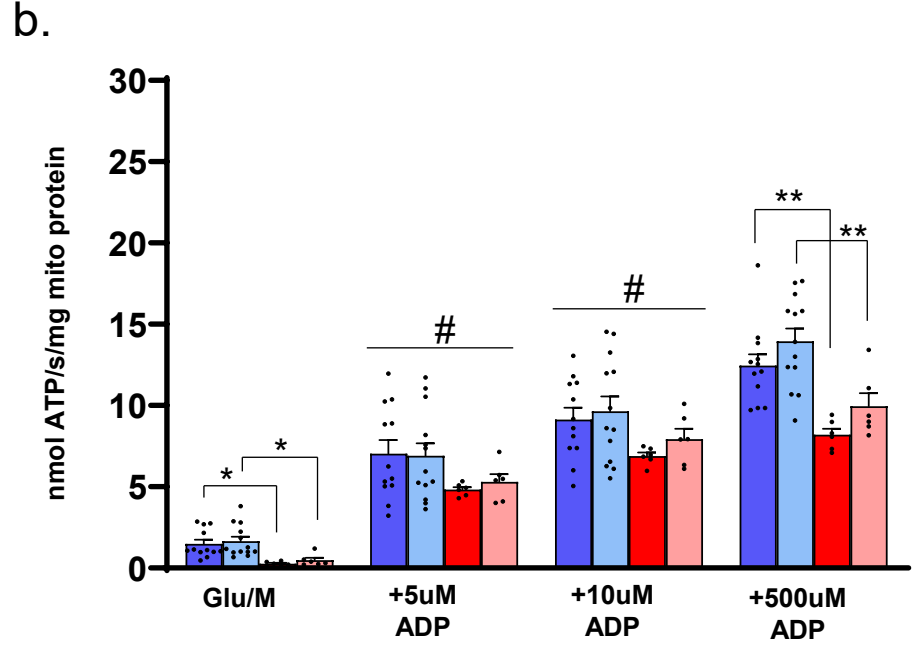
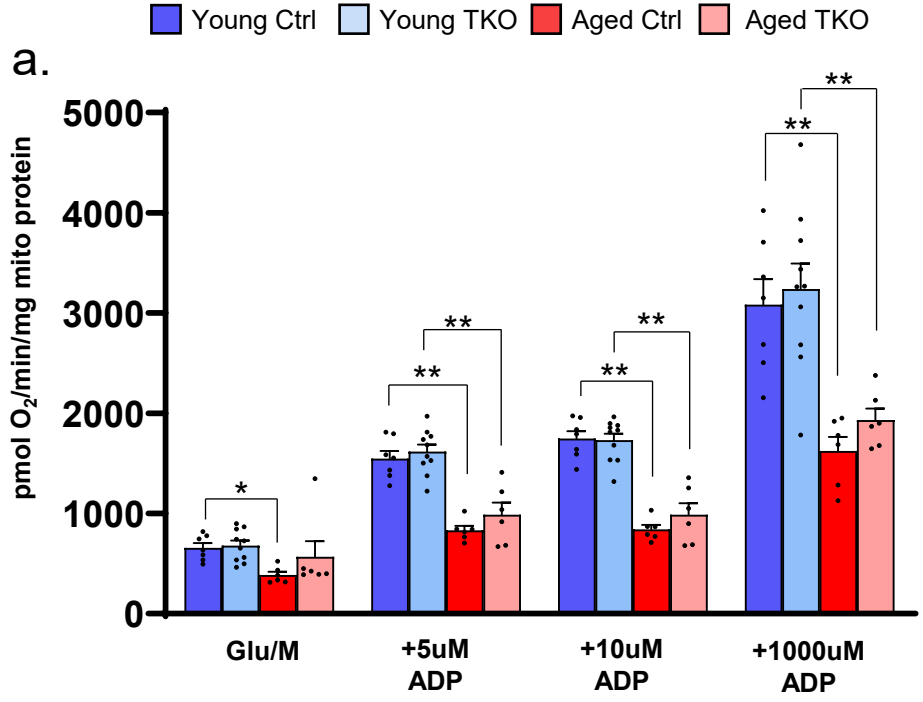


d.

Average Food Intake



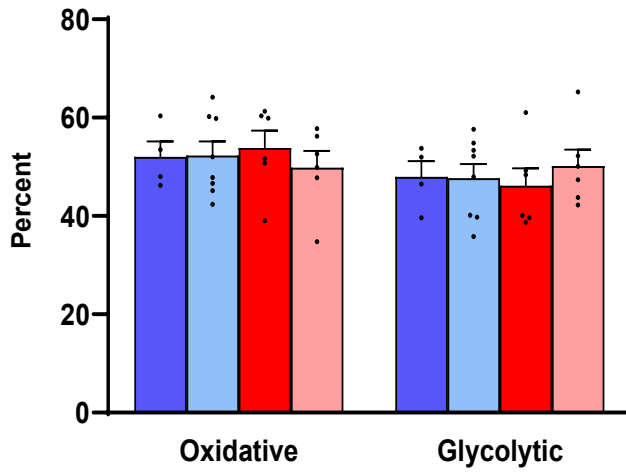
Supplemental Figure S6



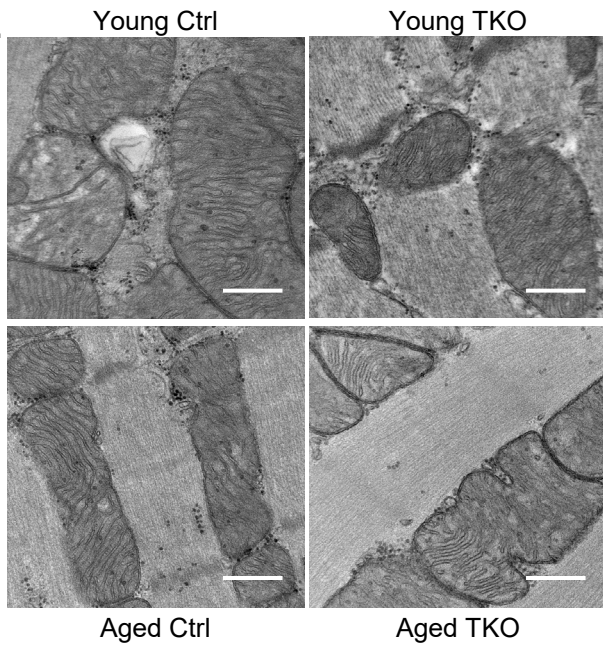
Supplemental Figure S7

■ Young Ctrl
 ■ Young TKO
 ■ Aged Ctrl
 ■ Aged TKO

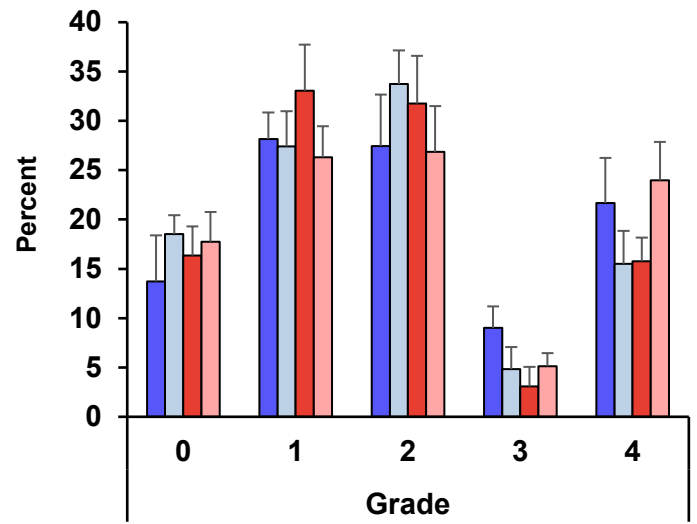
a.



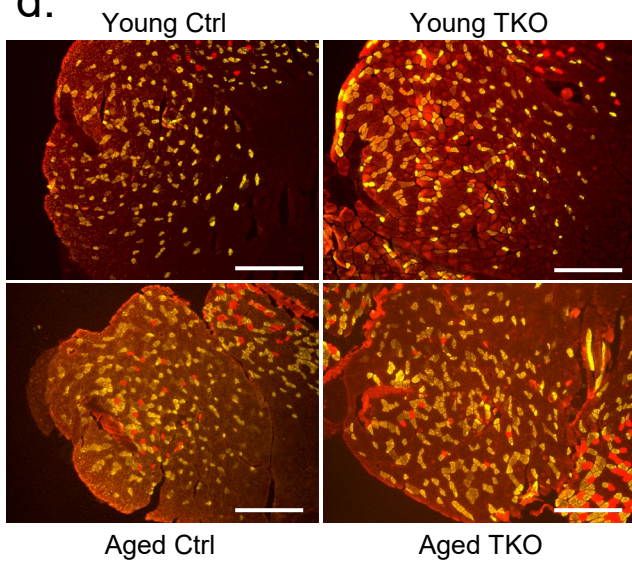
b.



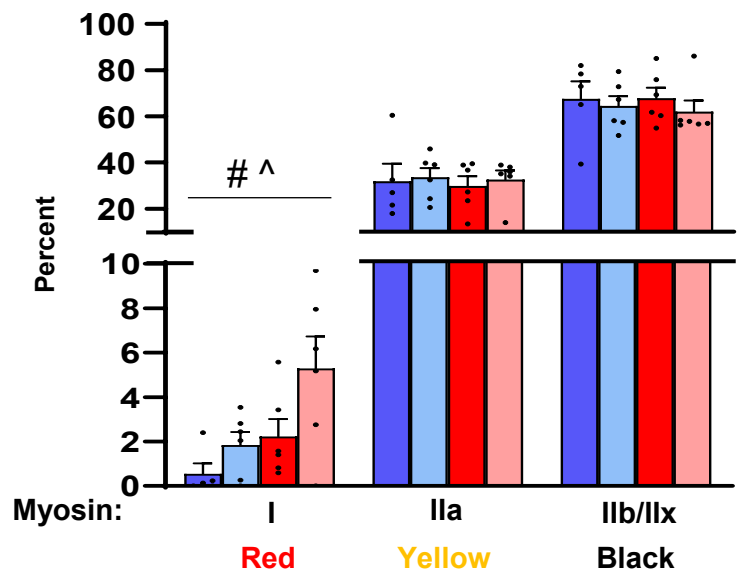
c.



d.



e.



Supplemental Figure S8

■ Young Ctrl
 ■ Young TKO
 ■ Aged Ctrl
 ■ Aged TKO

